Phonon-assisted Γ-X transfer in (001)-grown GaAs/AlAs superlattices

O. E. Raichev

Institute of Semiconductor Physics, Ukrainian Academy of Science, Prospekt Nauki 45, Kiev-28, 252650, Ukraine

A theory of phonon-assisted intervalley Γ-X transfer in periodic heterostructures GaAs/AlAs is developed on the basis of the envelope-function approximation. Matrix elements of intervalley transitions are expressed through the overlap integrals of Γ and X envelope functions with use of Γ-X intervalley deformation potential constants of bulk GaAs and AlAs. The phonon spectrum of an ideal GaAs/AlAs periodic heterostructure is studied in a microscopic approach. It is shown that phonons responsible for intervalley transitions are GaAs-like and AlAs-like X-point LO phonons, confined within GaAs and AlAs layers, respectively. Γ-X transfer times due to phonon-assisted scattering are calculated for the problem of photoexcited-electron relaxation in the type-II GaAs/AlAs superlattices and compared with the transfer times due to the phononless transition mechanism (Γ-X mixing). Both phonon-assisted Γ-X scattering and Γ-X mixing are important for the determination of Γ-X transfer times. The calculated values of Γ-X transfer times and their dependence on GaAs and AlAs layer thicknesses are in agreement with the experimental data.

I. INTRODUCTION

In GaAs/AlAs (or GaAs/Al$_x$Ga$_{1-x}$As, $x > 0.5$) heterostructures the Γ valley of GaAs and the X valley of AlAs (or Al$_x$Ga$_{1-x}$As) are the lowest energy valleys for the electrons. For this reason, electron transport phenomena in these structures often include electron transitions between GaAs and AlAs layers, accompanied by the intervalley Γ-X transfer (see Refs. 1 and 2 and references therein). Such transitions both in real space and in momentum space are the subject of studies in the past several years. It is necessary to take into account these transitions for the description of the real-space-transfer (RST) -induced negative differential conductance in GaAs/AlAs multilayer systems,[3,4] for the examination of relaxation of photoexcited electrons in the type-II GaAs/AlAs superlattices,[2] and for the calculations of the tunnel current in single-barrier,[5] double-barrier,[6] and multiquantum well[7,8] (MQW) GaAs/AlAs structures.

There are two principal mechanisms of the Γ-X transfer in GaAs/AlAs heterostructures. The first, known as Γ-X mixing, does not include any scattering processes and exists due to the nonorthogonality of the Γ-electron and X-electron wave functions in the heterostructure. In the envelope function approximation (EFA), this nonorthogonality is considered as the nonorthogonality of Bloch amplitudes (i.e., microscopic periodic parts) of Γ and X wave functions in the vicinity of the interfaces. As a result, boundary conditions for the envelope functions of Γ and X states include terms corresponding to the mixing of these states.[1,9] If the GaAs/AlAs heterostructure is assumed to be ideal (i.e., homogeneous along the layer planes), transitions by this mechanism occur with conservation of longitudinal component k of the electron wave vector. Therefore, Γ-X transfer by the Γ-X mixing mechanism occurs only in (001)-grown structures between Γ-valley states and X_z-valley states (here X_z is the valley oriented along the growth axis z).

The second mechanism of Γ-X transfer can be characterized as interlayer Γ-X scattering and implies bulklike intervalley scattering induced by the intervalley phonons[10] or alloy disorder[11,12] (provided that alloy-containing structure, for example, GaAs/Al$_x$Ga$_{1-x}$As, is considered). The probability of Γ-X scattering is not restricted by the k-conservation requirement. In (001)-grown structures electron transitions occur not only between the Γ valley and the X_z valley, but also between the Γ valley and two other X valleys X_x, X_y.

Although both of the above-mentioned transfer mechanisms are important, Γ-X mixing has been more extensively studied than Γ-X scattering. The examination of the phonon-assisted Γ-X transfer has been carried out in Ref. 10 with use of a simplified (bulk) model of the phonons. However, due to considerable difference in the atomic masses of Ga and Al, the lattice vibrational pattern of the GaAs/AlAs heterostructures significantly differs from the lattice vibrational pattern of bulk GaAs or AlAs. Therefore, any electron-phonon interaction in the heterostructures (including the interaction with intervalley phonons, which is responsible for the phonon-assisted Γ-X transfer) must be considered on the basis of more realistic models of the phonons.

In this work an analytical approach within the EFA is developed in order to calculate probabilities of the phonon-assisted electron scattering between Γ and $X_z, X_{x,y}$ valleys in GaAs/AlAs superlattices grown in the (001) direction. The case of the superlattice is chosen because of its importance in connection with the problem of high-speed Γ-X RST devices (Ref. 4, Sec. 3.9) and with the problem of photoexcited electrons relaxation in the type-II GaAs/AlAs superlattices.[2,13,14] It should be noted also that phonon-assisted Γ-X transfer (as well as any other transfer by Γ-X scattering mechanism) is especially

　　　<u>49</u>　　5448

important for the GaAs/AlAs superlattices and MQW's with quantized Γ and X electrons, because the rate of Γ-X mixing-induced transfer in these structures can be suppressed due to the k-conservation requirement. The importance of the phonon-assisted Γ-X transfer in GaAs/AlAs superlattices and MQW's has been revealed in many works. There was direct detection of nonequilibrium phonons generated during the Γ-X relaxation of photoexcited electrons.[14] Spectra of indirect photoluminescence from type-II GaAs/AlAs superlattices always exhibit phonon lines (see, for example, Ref. 15); these lines can be even more intensive than the zerophonon line concerned with Γ-X mixing (or elastic Γ-X scattering).

The paper is organized as follows. In Sec. II matrix elements of intervalley phonon-assisted Γ-X electron scattering in the GaAs/AlAs heterostructures are expressed through the overlap sums of the Γ-electron and the X-electron envelope functions with the amplitudes of lattice vibrations. In Sec. III the spectrum and the corresponding eigenfunctions of the lattice vibrations in the GaAs/AlAs superlattice are calculated from the microscopic model taking into account the short-range interatomic interaction for the first and second neighbors in the Born–von Karman approach and the long-range (Coulomb) interatomic interaction in the rigid-ion model. An expression for the phonon-assisted Γ-X transfer probability is derived in Sec. IV. We also calculated the Γ-X transfer times in application to the problem of photoexcited electrons relaxation in type-II superlattices and compared calculated values with the available experimental data.

II. MATRIX ELEMENTS
OF THE INTERVALLEY Γ-X SCATTERING
IN GaAs/AlAs HETEROSTRUCTURES

In order to calculate Γ-X transfer rates, we need to find matrix elements of intervalley transitions between the Γ-valley and the X-valley electron states. There are two groups of X valleys in (001)-grown GaAs/AlAs heterostructure: the X_z valley oriented along the heterostructure axis z and two side valleys X_x, X_y oriented along the x and y directions. The matrix element of Γ-X_x transition is equal to the matrix element of Γ-X_y transition because the X_x, X_y valleys are equivalent. We need to calculate the two following matrix elements:

$$M_{\lambda,\lambda'}^{\Gamma X_x}(\mathbf{k},\mathbf{k}') = \int \int d\mathbf{r}\, dz\, \Psi_{\lambda'\mathbf{k}'}^{X_x *}(\mathbf{r},z)\Psi_{\lambda\mathbf{k}}^{\Gamma}(\mathbf{r},z)\varphi(\mathbf{r},z) , \quad (1)$$

$$M_{\lambda,\lambda'}^{\Gamma X_z}(\mathbf{k},\mathbf{k}') = \int \int d\mathbf{r}\, dz\, \Psi_{\lambda'\mathbf{k}'}^{X_z *}(\mathbf{r},z)\Psi_{\lambda\mathbf{k}}^{\Gamma}(\mathbf{r},z)\varphi(\mathbf{r},z) , \quad (2)$$

where $\varphi(\mathbf{r},z)$ is the amplitude of the perturbation potential due to the lattice vibrations [the time-dependent perturbation potential is assumed to be equal to $\varphi(\mathbf{r},z)e^{-i\omega t}+\varphi^*(\mathbf{r},z)e^{i\omega t}$], $\mathbf{r}=(x,y)$, and $\Psi_{\lambda\mathbf{k}}^{i}(\mathbf{r},z)$ are the wave functions of the electron states described by the valley index $i=\Gamma,X_x,X_z$, longitudinal wave vector $\mathbf{k}$, and transverse quantum number λ. In the EFA $\Psi_{\lambda\mathbf{k}}^{i}(\mathbf{r},z)$ can be expressed as

$$\Psi_{\lambda\mathbf{k}}^{\Gamma}(\mathbf{r},z)=\frac{1}{\sqrt{S}}u_{\Gamma}(\mathbf{r},z)F_{\lambda\mathbf{k}}^{\Gamma}(z)\exp(i\mathbf{k}\cdot\mathbf{r}) ,$$

$$\Psi_{\lambda\mathbf{k}}^{X_x}(\mathbf{r},z)=\frac{1}{\sqrt{S}}u_{X_x}(\mathbf{r},z)F_{\lambda\mathbf{k}}^{X_x}(z)\exp\left[i\mathbf{k}\cdot\mathbf{r}+i\frac{\pi}{a}x\right] , \quad (3)$$

$$\Psi_{\lambda\mathbf{k}}^{X_z}(\mathbf{r},z)=\frac{1}{\sqrt{S}}u_{X_z}(\mathbf{r},z)F_{\lambda\mathbf{k}}^{X_z}(z)\exp\left[i\mathbf{k}\cdot\mathbf{r}+i\frac{\pi}{a}z\right] ,$$

where $F_{\lambda\mathbf{k}}^{i}(z)$ are the electron envelope functions, $u_i(\mathbf{r},z)$ are the Bloch amplitudes, $a=2.83$ Å is the monolayer width which is assumed to be the same for GaAs and AlAs, and S is the normalization square. The functions $u_i(\mathbf{r},z)$ conserve their bulk properties within each layer except small (1–2 monolayer wide) regions in the vicinity of interfaces. The envelope functions $F_{\lambda\mathbf{k}}^{i}(z)$ are slowly varying with coordinate z (i.e., do not change considerably on the microscopic scale). We should note that $|\mathbf{k}| \ll \pi/a$ in (3), because we consider electron states near the extrema of the Γ and X valleys.

In order to calculate matrix elements (1) and (2), we need to express $\varphi(\mathbf{r},z)$ through the amplitudes of atomic vibrations $d_{n,\alpha}^{s}$, where n is the number of primitive cell in the crystal, s denotes kind of atom in the cell, cation (C) or anion (A) (in our particular case A denotes As atoms and C denotes Ga or Al atoms), and α is the coordinate index (x,y,z). The most general linear relation between $\varphi(\mathbf{r},z)$ and $d_{n,\alpha}^{s}$ is

$$\varphi(\mathbf{r},z)=\sum_{n,s,\alpha} U_{s,\alpha}^{n}(\mathbf{r},z)d_{n,\alpha}^{s} , \quad (4)$$

where $U_{s,\alpha}^{n}(\mathbf{r},z)$ is the variation of the potential energy $\varphi(\mathbf{r},z)$ due to the displacement of atoms n,s along axis α. Summation over n in (4) implies summation over three integer numbers n_1, n_2, n_3. These numbers determine the vector of the atomic position $\mathbf{a}_n = n_1\mathbf{a}_1 + n_2\mathbf{a}_2 + n_3\mathbf{a}_3$, where $\mathbf{a}_1=(0,a,a), \mathbf{a}_2=(a,0,a)$, and $\mathbf{a}_3=(a,a,0)$ are the Bravais vectors of the fcc lattice. Due to translational symmetry in the (xy) plane we can rewrite $U_{s,\alpha}^{n}$ as $V_{s,\alpha}^{m}[x-a(n_2+n_3),y-a(n_1+n_3);z]$, where $m=n_1+n_2$ is the monolayer number in the z direction. We take into account periodicity of $u_i(\mathbf{r},z)$ in the (xy) plane and perform two dimensional (2D) Fourier transformations:

$$V_{s,\alpha}^{m}(x,y;z)=\frac{1}{S}\sum_{q_x',q_y'} V_{s,\alpha}^{m}(q_x',q_y';z)\exp(iq_x'x+iq_y'y) , \quad (5)$$

$$u_{\Gamma}(\mathbf{r},z)u_{X_{x,z}}^{*}(\mathbf{r},z)=\sum_{l_1',l_2'} w_{l_1',l_2'}^{\Gamma X_{x,z}}(z)\exp\left[i\frac{\pi}{a}[(l_1'-l_2')x + (l_1'+l_2')y]\right] , \quad (6)$$

$$d_{n,\alpha}^{s}=\sum_{q_x,q_y} A_{\alpha}^{s}(\mathbf{q},m)\exp[iq_x a(n_2+n_3)+iq_y a(n_1+n_3)] . \quad (7)$$

Here l_1, l_2, l_1', l_2' are the integer numbers connected with 2D reciprocal lattice of the system, $\mathbf{q}=(q_x,q_y)$. After substitution of Eqs. (3)–(7) into (1) and (2), we obtain

$$M_{\lambda,\lambda'}^{\Gamma X_x}(\mathbf{k},\mathbf{k}')$$

$$= \frac{1}{2a^2} \sum_{q_x,q_y} \sum_{l_1,l_2,l_1',l_2'} \delta_{k_x'-k_x,q_x+(\pi/a)(l_1'-l_2'-l_1+l_2-1)} \delta_{k_y'-k_y,q_y+(\pi/a)(l_1'+l_2'-l_1-l_2)}$$

$$\times \sum_{s,m,\alpha} (-1)^{m(l_1+l_2)} A_\alpha^s(\mathbf{q},m)$$

$$\times \int dz\, w_{l_1',l_2'}^{\Gamma X_x}(z) V_{s,\alpha}^m \left[q_x - \frac{\pi}{a}(l_1-l_2), q_y - \frac{\pi}{a}(l_1+l_2); z \right] F_{\lambda\mathbf{k}}^\Gamma(z) F_{\lambda'\mathbf{k}'}^{X_x\,*}(z) , \tag{8}$$

$$M_{\lambda,\lambda'}^{\Gamma X_z}(\mathbf{k},\mathbf{k}')$$

$$= \frac{1}{2a^2} \sum_{q_x,q_y} \sum_{l_1,l_2,l_1',l_2'} \delta_{k_x'-k_x,q_x+(\pi/a)(l_1'-l_2'-l_1+l_2)} \delta_{k_y'-k_y,q_y+(\pi/a)(l_1'+l_2'-l_1-l_2)}$$

$$\times \sum_{s,m,\alpha} (-1)^{m(l_1+l_2)} A_\alpha^s(\mathbf{q},m)$$

$$\times \int dz\, w_{l_1',l_2'}^{\Gamma X_z}(z) V_{s,\alpha}^m \left[q_x - \frac{\pi}{a}(l_1-l_2), q_y - \frac{\pi}{a}(l_1+l_2); z \right] F_{\lambda\mathbf{k}}^\Gamma(z) F_{\lambda'\mathbf{k}'}^{X_z\,*}(z) \exp\left[-i\frac{\pi}{a}z \right] . \tag{9}$$

To carry on our calculations, we represent $V_{s,\alpha}^m(q_x,q_y;z)$ as a sum of two parts:

$$V_{s,\alpha}^m(q_x,q_y;z) = V_{s,\alpha}^{m(l)}(q_x,q_y;z) + V_{s,\alpha}^{m(C)}(q_x,q_y;z) . \tag{10}$$

Here $V_{s,\alpha}^{m(C)}(q_x,q_y;z)$ is the long-range (Coulomb) part which is responsible for the existence of macroscopic electric fields and the Fröhlich electron-phonon interaction. This part can be described in the usual way from the rigid-ion approach. For example,

$$V_{s,x}^{m(C)}(q_x,q_y;z) = iq_x \frac{2\pi e_m^s}{\sqrt{q_x^2+q_y^2}} \exp(-iq_x\rho_x^s - iq_y\rho_y^s)$$

$$\times \exp(-\sqrt{q_x^2+q_y^2}\,|z-\rho_z^s-am|) , \tag{11}$$

where $(\rho_x^s,\rho_y^s,\rho_z^s)$ is the lattice basis vector [(0,0,0) for $s=A$ and $(a/2,a/2,a/2)$ for $s=C$] and e_m^s is the effective charge of the ion of kind s. The value of this charge changes between the bulk GaAs value and the bulk AlAs value in narrow regions near the interfaces. The remaining part $V_{s,\alpha}^{m(l)}(q_x,q_y;z)$ describes the local variation of the potential energy due to the lattice deformation. This part rapidly decreases with an increase of $|z-am|$. The typical spatial scale of this decrease is assumed to be small in comparison with the spatial scales of the envelope functions $F_{\lambda\mathbf{k}}^\Gamma(z)$, $F_{\lambda'\mathbf{k}'}^{X_x}(z)$, and $F_{\lambda'\mathbf{k}'}^{X_z}(z)$.

Consider the matrix element $M_{\lambda,\lambda'}^{\Gamma X_x}(\mathbf{k},\mathbf{k}')$. The momentum conservation laws represented by the δ symbols in Eq. (8) can be satisfied only for lattice vibrations with the longitudinal wave vector $\mathbf{q}=(\pi/a,0)+\tilde{\mathbf{q}}$ (or equivalent wave vectors in the extended Brillouin zone), where $\tilde{\mathbf{q}}=\mathbf{k}'-\mathbf{k}$, $|\tilde{\mathbf{q}}| \ll \pi/a$. For given $\mathbf{q}$, the Coulomb part of $V_{s,\alpha}^m$ from (8) decreases with increasing $|z-am|$ at least as fast as $\exp(-\pi/a|z-am|)$ [see (11)]. Therefore, $V_{s,\alpha}^m[q_x-(\pi/a)(l_1-l_2),q_y-(\pi/a)(l_1+l_2);z]$ in (8) rapidly decreases with increasing $|z-am|$, and we can re-

place the envelope-function product $F_{\lambda\mathbf{k}}^\Gamma(z)F_{\lambda'\mathbf{k}'}^{X_x\,*}(z)$ for $F_{\lambda\mathbf{k}}^\Gamma(ma)F_{\lambda'\mathbf{k}'}^{X_x\,*}(ma)$ and carry it out of the sign of integration. Neglecting also small corrections of order $\tilde{q}a/\pi$, we obtain

$$M_{\lambda,\lambda'}^{\Gamma X_x}(\mathbf{k},\mathbf{k}') = \sum_{\tilde{\mathbf{q}}} \delta_{\mathbf{k}'-\mathbf{k},\tilde{\mathbf{q}}} \sum_{s,m,\alpha} P_\alpha^s(m) F_{\lambda\mathbf{k}}^\Gamma(ma) F_{\lambda'\mathbf{k}'}^{X_x\,*}(ma)$$

$$\times A_\alpha^s[(\pi/a,0),m] , \tag{12}$$

where

$$P_\alpha^s(m) = \frac{1}{2a^2} \sum_{l_1,l_2} (-1)^{m(l_1+l_2)}$$

$$\times \int dz\, w_{l_1,l_2}^{\Gamma X_x}(z) V_{s,\alpha}^m \left[-\frac{\pi}{a}(l_1-l_2-1) , -\frac{\pi}{a}(l_1+l_2);z \right] . \tag{13}$$

In the limit of bulk crystal, $P_\alpha^s(m)$ is independent of m and proportional to the intervalley Γ-X deformation potential (DP) constant. In the heterostructure, taking into account above-mentioned local property of $V_{s,\alpha}^m[-(\pi/a)(l_1-l_2-1),-(\pi/a)(l_1+l_2);z]$ we obtain

$$P_x^C(m) = P(m) = \begin{cases} D_{1X}a\sqrt{M_{C1}/(M_{C1}+M_A)} , \\ \qquad m \in \text{GaAs layer} \\ D_{2X}a\sqrt{M_{C2}/(M_{C2}+M_A)} , \\ \qquad m \in \text{AlAs layer} \end{cases} \tag{14}$$

where M_{C1},M_{C2},M_A are the atomic masses of Ga, Al, and As and D_{1X} and D_{2X} are the Γ-X DP constants of bulk GaAs and AlAs, respectively,

$$P_y^C(m) = P_z^C(m) = P_\alpha^A(m) = 0 \ . \tag{15}$$

In order to obtain (14) and (15), we assumed that each layer of the heterostructure contains many ($\gg 1$) monolayers, so we had reason to neglect "interface" effects [i.e., deviation of $w_{l_1,l_2}^{\Gamma X_x}(z)$ and $V_{s,\alpha}^m(q_x, q_y; z)$ from their bulk values in the vicinity of the interfaces] in comparison with the "bulklike" effects. For example, selection rules (15) (valid for the bulk GaAs and AlAs) can be violated near the interfaces, but this violation is neglected. In the similar way, we should stress that function $P_x^C(m)$, of course, does not change from one layer to another as abruptly as it seems from (14). However, $P_x^C(m)$ can be considered as an abrupt function with respect to slowly varying envelope functions [it is the meaning of Eq. (14)].

Consider now the matrix element $M_{\lambda,\lambda'}^{\Gamma X_z}(\mathbf{k}, \mathbf{k}')$. The momentum selection rules allow the interaction for the vibrations with $\mathbf{q} = (0,0) + \bar{\mathbf{q}}$ (or equivalent). In this case the Coulomb part $V_{s,\alpha}^{m(C)}[q_x - (\pi/a)(l_1 - l_2)$, $q_y - (\pi/a)(l_1 + l_2); z]$ may depend on $|z - am|$ as $\exp(|\bar{\mathbf{q}}\| z - am|)$. The existence of such long-range fields leads to the Fröhlich interaction, but it is important only for the *intravalley* electron transitions. For intervalley transitions, the contribution from the long-range terms of $V_{s,\alpha}^{m(C)}$ in the matrix element (9) can be neglected because this contribution is approximately proportional to the integral $\int dz \, w_{0,0}^{\Gamma X_z}(z) \exp[-i(\pi/a)z]$, which is equal to zero due to the Γ and X Bloch function orthogonality. Since the long-range terms are not important, $V_{s,\alpha}^m[q_x - (\pi/a)(l_1 - l_2), q_y - (\pi/a)(l_1 + l_2); z]$ can be considered as local. In a way similar to the Γ-X_x case we obtain

$$M_{\lambda,\lambda'}^{\Gamma X_z}(\mathbf{k}, \mathbf{k}') = \sum_{\bar{\mathbf{q}}} \delta_{\mathbf{k}' - \mathbf{k}, \bar{\mathbf{q}}} \sum_{s,m,\alpha} R_\alpha^s(m) F_{\lambda \mathbf{k}}^\Gamma(ma) F_{\lambda' \mathbf{k}'}^{X_z *}(ma)$$
$$\times A_\alpha^s[(0,0), m](-1)^m \ , \tag{16}$$

where

$$R_\alpha^s(m) = \frac{1}{2a^2} \sum_{l_1, l_2} (-1)^{m(l_1 + l_2 + 1)} \int dz \, w_{l_1, l_2}^{\Gamma X_z}(z) \ ,$$

$$V_{s,\alpha}^m \left[-\frac{\pi}{a}(l_1 - l_2), -\frac{\pi}{a}(l_1 + l_2); x \right] \exp\left[-i\frac{\pi}{a}z \right] \ . \tag{17}$$

After comparison of (16) and (17) with the bulk limit, we find

$$R_z^C(m) = P(m), \quad R_x^C(m) = R_y^C(m) = R_\alpha^A(m) = 0 \ . \tag{18}$$

In conclusion, we have expressed matrix elements of the phonon-assisted intervalley Γ-X_x and Γ-X_z electron transitions in the heterostructures through the bulk intervalley DP constants. The matrix elements are proportional to the overlap sums of electron envelope functions and amplitudes of the lattice vibrations with 2D wave vectors $\mathbf{q} = (\pi/a, 0)$ and $(0,0)$. In the following section we will consider lattice vibrations in GaAs/AlAs heterostructures in order to determine these amplitudes.

III. SPECTRUM OF LATTICE VIBRATIONS IN GaAs/AlAs SUPERLATTICES

In this section we develop a microscopic approach in order to calculate the vibrational spectrum and amplitudes of the atomic displacements $A_\alpha^s(\mathbf{q}, m)$ for the periodic GaAs/AlAs systems (superlattices or MQWs). We start from the dynamic equation for the atomic displacements

$$\omega^2 M_s^m d_{n,\alpha} = \sum_{n',\alpha',s'} \Phi_{\alpha,\alpha'}^{s,s'} \begin{vmatrix} n_1, n_1' \\ n_2, n_2' \\ n_3, n_3' \end{vmatrix} d_{n',\alpha'}^{s'} \ , \tag{19}$$

where Φ is the real-space force constant matrix, ω is the frequency of the lattice vibrations, and M_s^m is the mass of atom s (in our case $M_C^m = M_{C1}$ for $m \in$ GaAs and $M_C^m = M_{C2}$ for $m \in$ AlAs, $M_A^m = M_A$). After the substitution of (7) into (19) we obtain

$$\omega^2 M_s^m A_\alpha^s(\mathbf{q}, m) = \sum_{\substack{m',\alpha',s' \\ \text{even } m'-m}} \Phi_{\alpha,\alpha'}^{s,s'(e)}(\mathbf{q}; m, m') A_{\alpha'}^{s'}(\mathbf{q}, m')$$
$$+ \sum_{\substack{m',\alpha',s' \\ \text{odd } m'-m}} \Phi_{\alpha,\alpha'}^{s,s'(o)}(\mathbf{q}; m, m') A_{\alpha'}^{s'}(\mathbf{q}, m') \ , \tag{20}$$

where $m = n_1 + n_2$ and $m' = n_1' + n_2'$ are the monolayer numbers and $\Phi_{\alpha,\alpha'}^{s,s'(e,o)}(\mathbf{q}; m, m')$ are the interlayer force constants defined by the equations

$$\Phi_{\alpha,\alpha'}^{s,s'(e,o)}(\mathbf{q}; m, m') = \sum_{l_1(e,o)} \sum_{l_2} \Phi_{\alpha,\alpha'}^{s,s'} \begin{vmatrix} n_1, n_1' \\ n_2, n_2' \\ n_3, n_3' \end{vmatrix} \exp\left[ia(q_x + q_y)l_2 + i\frac{a}{2}(q_y - q_x)l_1 + i\frac{a}{2}(q_x + q_y)(m' - m) \right] \ . \tag{21}$$

Here $l_2 = n_3' - n_3$ and $l_1 = n_2' - n_1' - n_2 + n_1$ [due to the homogeneity in the plane (xy), the real-space force constant matrix depends only on l_1, l_2, m, m']. Index (e) or (o) at the first sum in (21) implies summation over either even l_1 or odd l_1, respectively.

Solutions of Eq. (20) are the amplitudes $A_{\alpha,j}^s(\mathbf{q}, m)$ and frequencies $\omega_j(\mathbf{q})$ of vibrational eigenmodes and j is the mode number. To proceed from the classical description of lattice vibrations to the phonons, we should normalize these amplitudes according to the equation

$$\sum_{m,\alpha,s} M_s^m A_{\alpha,j}^s(\mathbf{q},m) A_{\alpha,j'}^{s*}(\mathbf{q},m) = \delta_{j,j'} \frac{\hbar a^2}{S\omega_j(\mathbf{q})} \quad . \quad (22)$$

In order to calculate the matrix elements of the Γ-X transitions, we need to determine the amplitudes $A_{\alpha,j}^s(\mathbf{q},m)$ from (20) for certain $\mathbf{q}$. The solution of Eq. (20) [or (19)] is the subject of the microscopic theory of lattice vibrations in the heterostructures. Microscopic calculation of the lattice vibrations in GaAs/AlAs superlattices has been carried out in a number of works. In the first work[16] the linear chain model with first-neighbor interatomic interactions has been considered. Further works involved more sophisticated approaches: a first-neighbor bond-charge model with long-range interactions treated as a perturbation[17] and numerical calculations using a wide set of *ab initio* determined force constants.[18-21] Calculations[18-21] seem to be very accurate. On the other hand, one- or two-nearest-neighbor approximations allow us to use the idea of complex phonon band structure[17,22] and to carry out an almost analytical consideration for high-symmetry points.

The approach used in this work can be described as follows. We take into account the interaction between the first- and second-neighboring atoms in the most general way (the Born–von Karman approach) and the Coulomb interaction in rigid-ion model. This approach, in general, assumes the introduction of 22 bulk constants (11 for each material): two effective ionic charges, four first-neighbor constants and sixteen second-neighbor constants, plus a number of "interface constants" for the description of interatomic interaction near the interfaces. To make calculations easier and to avoid the introduction of interface constants, we also assumed that all bulk constants of GaAs are equal to the corresponding bulk constants of AlAs. This assumption is known as "mass approximation"[18] because the only difference between GaAs and AlAs in the dynamical equations is the difference in the atomic masses of Ga and Al. Mass approximation works rather well[18,20,23] due to the similarity in the nature of the bonding in GaAs and AlAs and can be improved by the assumption of different effective ionic charges ("mass and charge approximation"). In the mass approximation the number of constants is reduced to 11. To calculate $A_\alpha^s(\mathbf{q},m)$ for $\mathbf{q}=(\pi/a,0)$ and $(0,0)$, we actually need 9 constants. These constants have been determined by fitting the calculated bulk phonon frequencies in the Γ, X, and W points to the experimental values summarized in Ref. 23. LO_Γ, TO_Γ, LO_X, LA_X, TO_X, TA_X, and LA_W frequencies of GaAs and TA_X and TO_W frequencies of AlAs were chosen for the exact fit.

Consider vibrations with $\mathbf{q}=(\pi/a,0)$. Due to large absolute value of $\mathbf{q}$, the Coulomb part of the interlayer forces rapidly decreases with increasing $|m'-m|$. With high accuracy, the range of the Coulomb interaction can be restricted by one monolayer. Therefore, we add the Coulomb part to the short-range part (first- and second-neighbor forces) and obtain first- and second-neighbor problem with the renormalized Born–von Karman constants. For given $\mathbf{q}$, the system of equations (20) splits into two independent subsystems for the amplitudes $A_x^C(\mathbf{q},m)$, $A_y^C(\mathbf{q},m)$, $A_z^A(\mathbf{q},m)$ and $A_x^A(\mathbf{q},m)$, $A_y^A(\mathbf{q},m)$,

$A_z^C(\mathbf{q},m)$. We will consider only the first subsystem because only cationic motion in the x direction [$A_x^C(\mathbf{q},m)$] contributes in $M_{\lambda,\lambda'}^{\Gamma X_x}(\mathbf{k},\mathbf{k}')$. The subsystem can be written in the following way:

$$C(m)\hat{I} A_\beta(m) = \frac{1}{2} \begin{vmatrix} -G & H \\ -H & G \end{vmatrix} A_\beta(m-1)$$
$$+ \frac{1}{2} \begin{vmatrix} -G & -H \\ H & G \end{vmatrix} A_\beta(m+1) , \quad (23)$$

where $A_\beta(m) = A_\beta^C[(\pi/a,0),m]$, $\beta=x,y$, and $\hat{I}$ is the unit matrix

$$A_z^A[(\pi/a,0),m] = -\frac{2\tilde{\gamma}}{D}[A_x(m) + A_y(m)$$
$$- A_x(m-1) + A_y(m-1)] , \quad (24)$$

$$C(m) = D(M_C^m \omega^2 - 4\tilde{\alpha} - 12\tilde{\alpha}_C - 4\tilde{\beta}_C) - 8\tilde{\gamma}^2$$

$[C(m) = C_1$ for $m \in \text{GaAs}$, $C(m) = C_2$ for $m \in \text{AlAs}]$,
$$(25)$$

$$G = 8\tilde{\gamma}^2 - 4D(\tilde{\alpha}_C - \tilde{\beta}_C), \quad H = 8\tilde{\gamma}^2 - 4D\tilde{\delta}_C , \quad (26)$$

$$D = \omega^2 M_A - (4\tilde{\alpha} + 8\tilde{\alpha}_A + 8\tilde{\beta}_A) . \quad (27)$$

In (24)–(27) $\tilde{\alpha}=4.05$, $\tilde{\gamma}=2.82$, $\tilde{\alpha}_A=0.397$, $\tilde{\alpha}_C=0.479$, $\tilde{\beta}_A=0.375$, $\tilde{\beta}_C=-1.333$, and $\tilde{\delta}_C=0.624$ are the renormalized Born–von Karman constants fitted as explained above (all values are given in 10^4 dyn/cm). The solution of the system (23) is

$$A_\beta(m) = A_i^+ \begin{bmatrix} 1 \\ \lambda_i \end{bmatrix} \exp(iq_i am) + A_i^- \begin{bmatrix} 1 \\ -\lambda_i \end{bmatrix} \exp(-iq_i am)$$
$$+ B_i^+ \begin{bmatrix} \lambda_i \\ 1 \end{bmatrix} (-1)^m \exp(iq_i am)$$
$$+ B_i^- \begin{bmatrix} -\lambda_i \\ 1 \end{bmatrix} (-1)^m \exp(-iq_i am) , \quad (28)$$

where $i=1$ for $m \in \text{GaAs}$ layer and $i=2$ for $m \in \text{AlAs}$ layer. Complex wave numbers q_1, q_2 are determined by the equations

$$\sin^2(q_{1,2}a) = \frac{C_{1,2}^2 - G^2}{H^2 - G^2} \quad . \quad (29)$$

Real solutions q_1 and q_2 of Eq. (29) correspond to the phonon spectrum along the X-W direction in bulk GaAs and AlAs, respectively. In the general case of complex q_1, q_2, Eq. (29) represents the complex dispersion relations. Depending on the values of the right-hand side, wave numbers q_1, q_2 may be real, pure imaginary, or complex with the real part equal to $\pi/2$. The values λ_1, λ_2 describe the polarization of the atomic motion. These values are determined by the equation

$$\lambda_{1,2} = \frac{iH \sin(q_{1,2}a)}{C_{1,2} - G \cos(q_{1,2}a)} \quad . \quad (30)$$

Eight constants $A_1^+, A_1^-, B_1^+, B_1^-, A_2^+, A_2^-, B_2^+, B_2^-$

must be found from the boundary conditions. Consider a superlattice $(GaAs)_{M_1}/(AlAs)_{M_2}$, where M_1 and M_2 are the numbers of monolayers in GaAs and AlAs layers, respectively. The number m is assumed to be counted from one of the interfaces, $m = 0, 1, \ldots, M_2 - 1 \in AlAs$, $m = -1, -2, \ldots, -M_1 \in GaAs$. Boundary conditions for this structure [see Eqs. (A1)–(A5) in the Appendix] represent an 8×8 linear system of equations for the determination of vibrational eigenmodes (frequency eigenvalues and corresponding pattern of atomic displacements) of the superlattice. These modes are described by the transverse wave number Q and the miniband number N [$j = (N, Q)$]. Calculation shows that only solutions with real q_1 (GaAs-like modes), or real q_2 (AlAs-like modes), or both real q_1 and q_2 (mixed modes) satisfy the boundary conditions. Solutions with both complex q_1 and q_2 (interfacelike modes) appear to be forbidden. Since discrete frequencies $\omega_{NQ}(q)$ are situated inside bulk frequency regions, every solution is bound to the proper frequency region: LO, TO, or TA. Calculation also reveals that the spectrum is sensitive to the parity of M_1 and M_2. For odd M_1 (M_2) GaAs (AlAs) -like states form pairs with almost equal frequencies [this degeneration is exact for single-layer structures: GaAs (AlAs) layers in the AlAs (GaAs) matrix]. Amplitudes of vibrations for each such pair (N, N') obey the relations

$$A_{x,N'Q}(m) \simeq -(-1)^m A_{y,NQ}(m) \, ,$$
$$A_{y,N'Q}(m) \cong -(-1)^m A_{x,NQ}(m) \, . \tag{31}$$

In the case of even M_1 (M_2) GaAs (AlAs) -like states are nondegenerate and

$$A_{y,NQ}(m) \cong \pm(-1)^m A_{x,NQ}(m) \tag{32}$$

for each mode. Approximate relations (31) and (32) are exact for single-layer structures.

Calculated amplitudes of the cationic displacements in $(GaAs)_8/(AlAs)_9$ superlattice at $q = (\pi/a, 0)$, $Q = 0$ are plotted in Fig. 1.[24] Several modes with smallest real q_1 bound to LO, TO, and TA regions of GaAs) or smallest real q_2 (bound to LO, TO, and TA regions of AlAs) are shown. In LO and TO regions GaAs (AlAs) -like modes are strongly evanescent in AlAs (GaAs) layers. In wide-layer limit $(M_1, M_2 \gg 1)$ these modes are almost the same as for single layers. Superlattice effects (including the dependence of mode frequency on Q) are negligible for these modes. On the other hand, modes in the TA region exhibit considerable penetration in both layers. Not only confined GaAs (AlAs) -like modes but also mixed modes exist in this region. It is worth noting that $A_{x,NQ}^C[(\pi/a,0),m]$ and $(-1)^m A_{y,NQ}^C[(\pi/a,0),m]$ for LO-bound AlAs-like modes can be well approximated by the functions $\sin(\pi L m /M_2)$, $L = 1, 2, \ldots$ [see Fig. 1(a)]. In a similar way, $A_{x,NQ}^C[(\pi/a,0),m]$ and $(-1)^m A_{y,NQ}^C[(\pi/a,0),m]$ for LO-bound GaAs-like modes can be approximated by the functions $\sin(\pi L m /M_1)$, if we detach the fast-oscillating contribution proportional to λ_1 [see Eq. (28)]. This contribution appeared to be not very small in our model even for

modes with smallest real q_1.

In order to calculate $M_{\lambda,\lambda'}^{\Gamma X_z}(k, k')$, we need to consider vibrations with small q. Generally speaking, we cannot examine these vibrations taking exactly $q = (0,0)$ instead of $q = \bar{q}$, even for $\bar{q} \to 0$. The reason lies in nonanalytical behavior of Coulomb interaction forces at small $\bar{q}$. Apart from the short-range forces (which can be taken into account by the renormalization of first- and second-neighbor Born–von Karman constants), the Coulomb part of interlayer force matrix $\Phi_{\alpha,\alpha'}^{s,s'(e,o)}(q; m, m')$ contains long-range forces decreasing with $|m' - m|$ as $\exp(|\bar{q}|a|m' - m|)$. Although the absolute values of these forces go to zero at $\bar{q} \to 0$, the effective range of interactions goes to infinity. It is nonanalyticity that is responsible for the existence of macroscopic vibrational modes localized at the interfaces. In our particular case, however, the long-range contribution in the Coulomb interlayer force matrix can be neglected because we search mostly for vibrational modes whose amplitudes oscillate with m on a microscopic scale [only these modes are significant for Γ-X_z scattering, see Eq. (16)]. We again reduce our task to first- and second-neighbor problem with renormalized Born–von Karman constants and put $q = (0,0)$.

For $q = (0,0)$, system (20) splits into two independent subsystems for the amplitudes $A_z^C(q, m)$, $A_z^A(q, m)$ and $A_x^C(q, m)$, $A_y^C(q, m)$, $A_x^A(qm)$, $A_y^A(q, m)$. We need to consider only the first subsystem:

$$\begin{bmatrix} C_A & -\bar{\alpha}/2 \\ -\bar{\alpha}/2 & C_C(m) \end{bmatrix} A^s(m) = \frac{1}{4} \begin{bmatrix} \bar{\alpha}_A & 2\bar{\alpha} \\ 0 & \bar{\alpha}_C \end{bmatrix} A^s(m-1)$$
$$+ \frac{1}{4} \begin{bmatrix} \bar{\alpha}_A & 0 \\ 2\bar{\alpha} & \bar{\alpha}_C \end{bmatrix} A^s(m+1) \, , \tag{33}$$

where $A^s(m) = A_z^s[(0,0), m], s = A, C$;

$$C_A = -M_A \omega^2 + \bar{\alpha} + \bar{\alpha}_A /2 \, ,$$
$$C_C(m) = -M_C^m \omega^2 + \bar{\alpha} + \bar{\alpha}_C /2 \, . \tag{34}$$

Here $\bar{\alpha} = 1.841 \times 10^5$ dyn/cm, $\bar{\alpha}_A = 0.412 \times 10^5$ dyn/cm, and $\bar{\alpha}_C = 0.544 \times 10^5$ dyn/cm. The solution of (33) is

$$A^s(m) = A_i^+ \begin{bmatrix} \lambda_i^+ \exp(-iq_i^+ a /2) \\ 1 \end{bmatrix} \exp(iq_i^+ am)$$
$$+ A_i^- \begin{bmatrix} \lambda_i^+ \exp(iq_i^+ a /2) \\ 1 \end{bmatrix} \exp(-iq_i^+ am)$$
$$+ B_i^+ \begin{bmatrix} \lambda_i^- \exp(-iq_i^- a /2) \\ 1 \end{bmatrix} \exp(iq_i^- am)$$
$$+ B_i^- \begin{bmatrix} \lambda_i^- \exp(iq_i^- a /2) \\ 1 \end{bmatrix} \exp(-iq_i^- am) \, , \tag{35}$$

$i = 1$ for $m \in GaAs$, and $i = 2$ for $m \in AlAs$. Four complex wave numbers q_1^+ and q_1^-, q_2^+ and q_2^- are the roots of the complex dispersion relations

$$\bar{\alpha}_A\bar{\alpha}_C\sin^4(q_{1,2}a/2)+[\bar{\alpha}^2+\bar{\alpha}(\bar{\alpha}_A+\bar{\alpha}_C)$$

$$-\omega^2(M_{C1,2}\bar{\alpha}_A+M_A\bar{\alpha}_C)]\sin^2(q_{1,2}a/2)$$

$$+\omega^2[\omega^2M_{C1,2}M_A-\bar{\alpha}(M_{C1,2}+M_A)]=0 \quad (36)$$

(two roots for each layer). Real solutions q_1 (q_2) of (36) describe bulk GaAs (AlAs) LO and LA phonon spectrum along the Γ-X direction. In the frequency regions where real roots exist, second roots are pure imaginary. These imaginary roots have large absolute values (of order π/a)
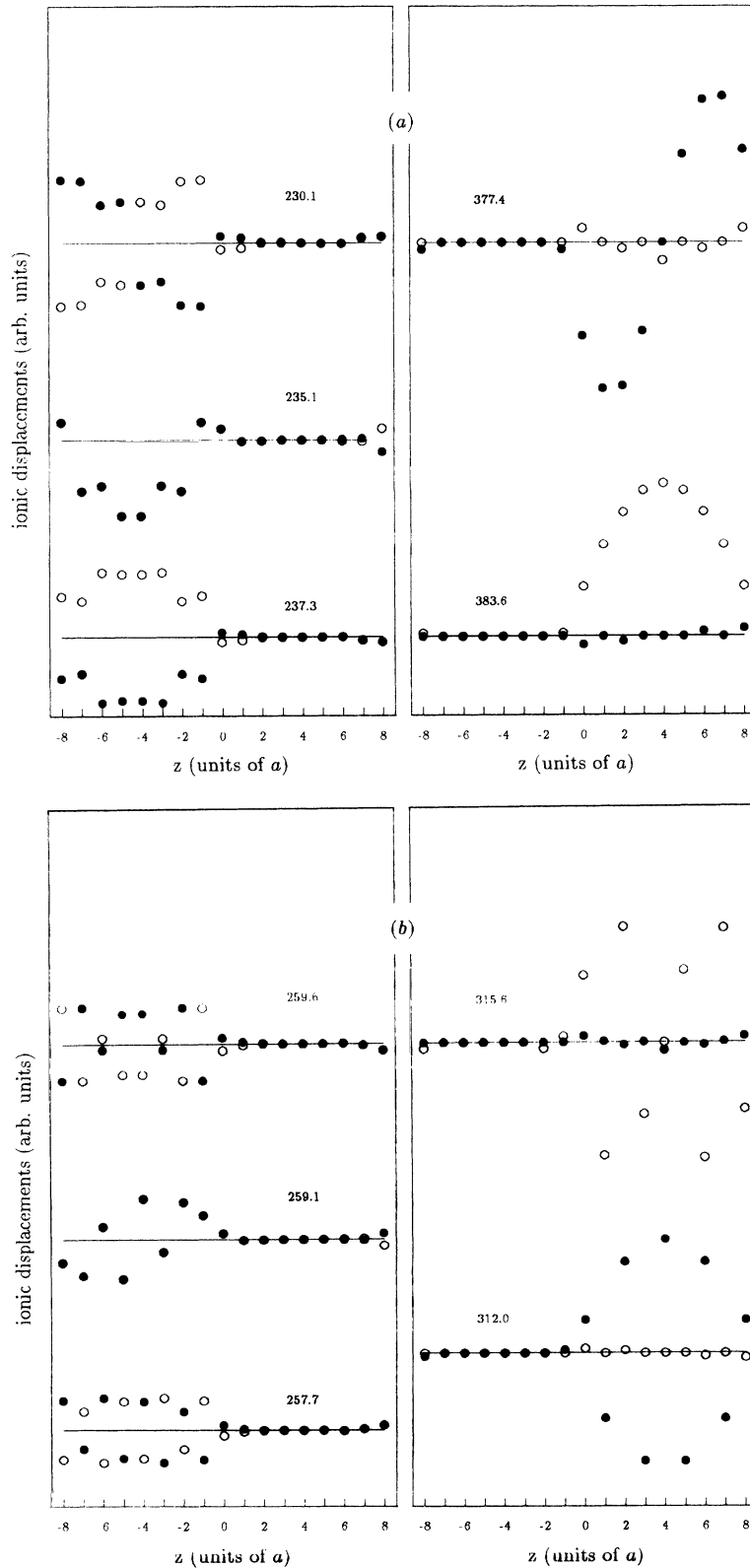
FIG. 1. The amplitudes of cationic displacements along the x and y directions in $(GaAs)_8/(AlAs)_9$ superlattice for the vibrations with $\mathbf{q}=(\pi/a,0)$, $Q=0$. Several modes bound to (a) LO, (b) TO, and (c) TA bands are shown. Empty circles, $A^C_{x,NQ}[(\pi/a,0),m]$; filled circles, $(-1)^m A^C_{y,NQ}[(\pi/a,0),m]$. Figures near each graph are corresponding mode frequencies $\omega_{NQ}(\pi/a,0)$ in cm^{-1}.
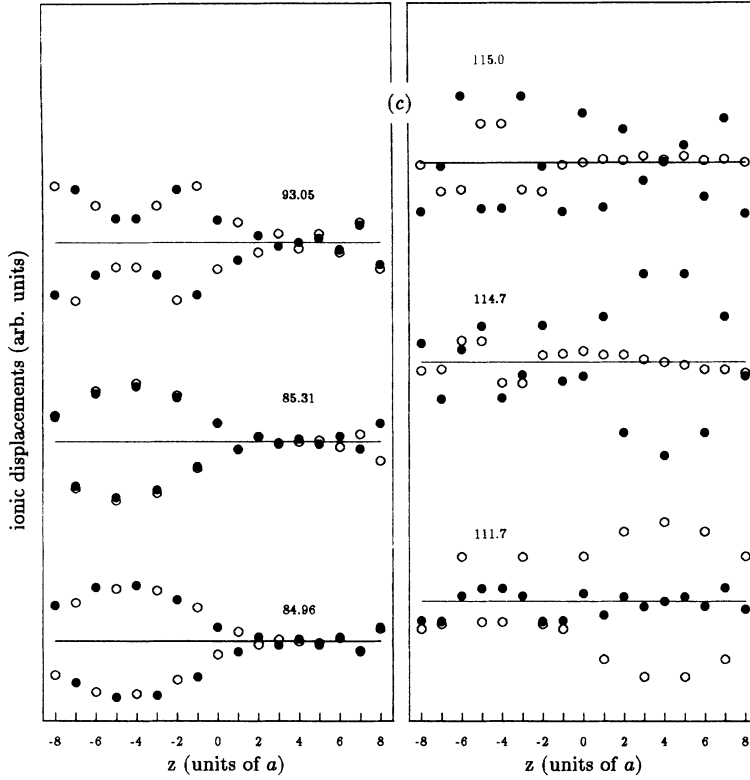
FIG. 1. (Continued).

and correspond to strongly evanescent contribution in (35). This contribution is important only in a close vicinity of the interfaces. We note that such roots do not appear in first-neighbor-interaction model of lattice vibrations.[16]

The values $\lambda_1^{\pm}$ and $\lambda_2^{\pm}$ are given by

$$\lambda_1^{\pm} = \frac{\bar{a}\cos(q_1^{\pm}a/2)}{C_A - 0.5\bar{a}_A\cos(q_1^{\pm}a)},$$

$$\lambda_2^{\pm} = \frac{\bar{a}\cos(q_2^{\pm}a/2)}{C_A - 0.5\bar{a}_A\cos(q_2^{\pm}a)}.$$

(37)

Boundary conditions for the determination of the spectrum and displacements are given in the Appendix [(A6)–(A10)].

The solutions of (33) are confined GaAs-like and AlAs-like modes bound to LO frequency regions and mixed modes in the LA frequency region. There are no interfacelike modes detected. The calculated amplitudes of the atomic displacements in the $(GaAs)_8/(AlAs)_9$ su-

perlattice for several modes with $\mathbf{q}=(0,0)$ and largest real q_1 or q_2 are shown in Fig. 2. We can see from Fig. 2(a) that $(-1)^m A_{z,NQ}^C[(0,0),m]$ for LO-bound GaAs- and AlAs-like modes can be approximated by the functions $\sin(\pi Lm/M_1)$ and $\sin(\pi Lm/M_2)$, $L=1,2,\ldots$. Mixed modes in the LA region are shown in Fig. 2(b). Displacements of anions $(-1)^m A_{z,NQ}^A[(0,0),m]$ are also plotted here in order to compare them with the displacements of cations.

IV. CALCULATION
OF THE Γ-X TRANSFER PROBABILITIES

Summarizing the results obtained in the Secs. II and III, we can derive the expression for the probability of the phonon-assisted Γ-X transfer. Partial probabilities $W_{\lambda,\lambda'}^{\Gamma X_x(\pm)}(\mathbf{k},\mathbf{k}')$ and $W_{\lambda,\lambda'}^{\Gamma X_z(\pm)}(\mathbf{k},\mathbf{k}')$ of electron scattering from the state $\Gamma,\lambda,\mathbf{k}$ to the state $X_x,\lambda',\mathbf{k}'$ or $X_z,\lambda',\mathbf{k}'$ due to emission (+) or absorption (−) of phonons are given by the equations

$$W_{\lambda,\lambda'}^{\Gamma X_x(\pm)}(\mathbf{k},\mathbf{k}') = \frac{2\pi}{\hbar}\sum_j \left|\sum_m P(m)A_{x,j}^C[(\pi/a,0),m]F_{\lambda\mathbf{k}}^{\Gamma}(ma)F_{\lambda'\mathbf{k}'}^{X_x*}(ma)\right|^2$$

$$\times [N_j(\pi/a,0)+\tfrac{1}{2}\pm\tfrac{1}{2}]\delta(\epsilon_{\lambda}^{\Gamma}(\mathbf{k})-\epsilon_{\lambda'}^{X_x}(\mathbf{k}')\mp\hbar\omega_j(\pi/a,0)),$$

(38)

$$W_{\lambda,\lambda'}^{\Gamma X_z(\pm)}(\mathbf{k},\mathbf{k}') = \frac{2\pi}{\hbar}\sum_j \left|\sum_m P(m)(-1)^m A_{z,j}^C[(0,0),m]F_{\lambda\mathbf{k}}^{\Gamma}(ma)F_{\lambda'\mathbf{k}'}^{X_z*}(ma)\right|^2$$

$$\times [N_j(0,0)+\tfrac{1}{2}\pm\tfrac{1}{2}]\delta(\epsilon_{\lambda}^{\Gamma}(\mathbf{k})-\epsilon_{\lambda'}^{X_z}(\mathbf{k}')\mp\hbar\omega_j(0,0)),$$

(39)

where $\epsilon_\lambda^\Gamma(\mathbf{k}), \epsilon_{\lambda'}^{X_x}(\mathbf{k}'), \epsilon_{\lambda'}^{X_z}(\mathbf{k}')$, are the energies of the Γ-valley and X_x, X_z-valley electron states, $N_j(\mathbf{q}) = \{\exp[\hbar\omega_j(\mathbf{q})/T] - 1\}^{-1}$ are the phonon occupation numbers, and T is the lattice temperature. Amplitudes of the atomic vibrations are assumed to be normalized by

Eq. (22). Expressions (38) and (39) (with proper spectra, envelope functions, and amplitudes of atomic displacements) are valid for any GaAs/AlAs heterostructure grown in the (001) direction.

Consider the case of the superlattice or MQW struc-
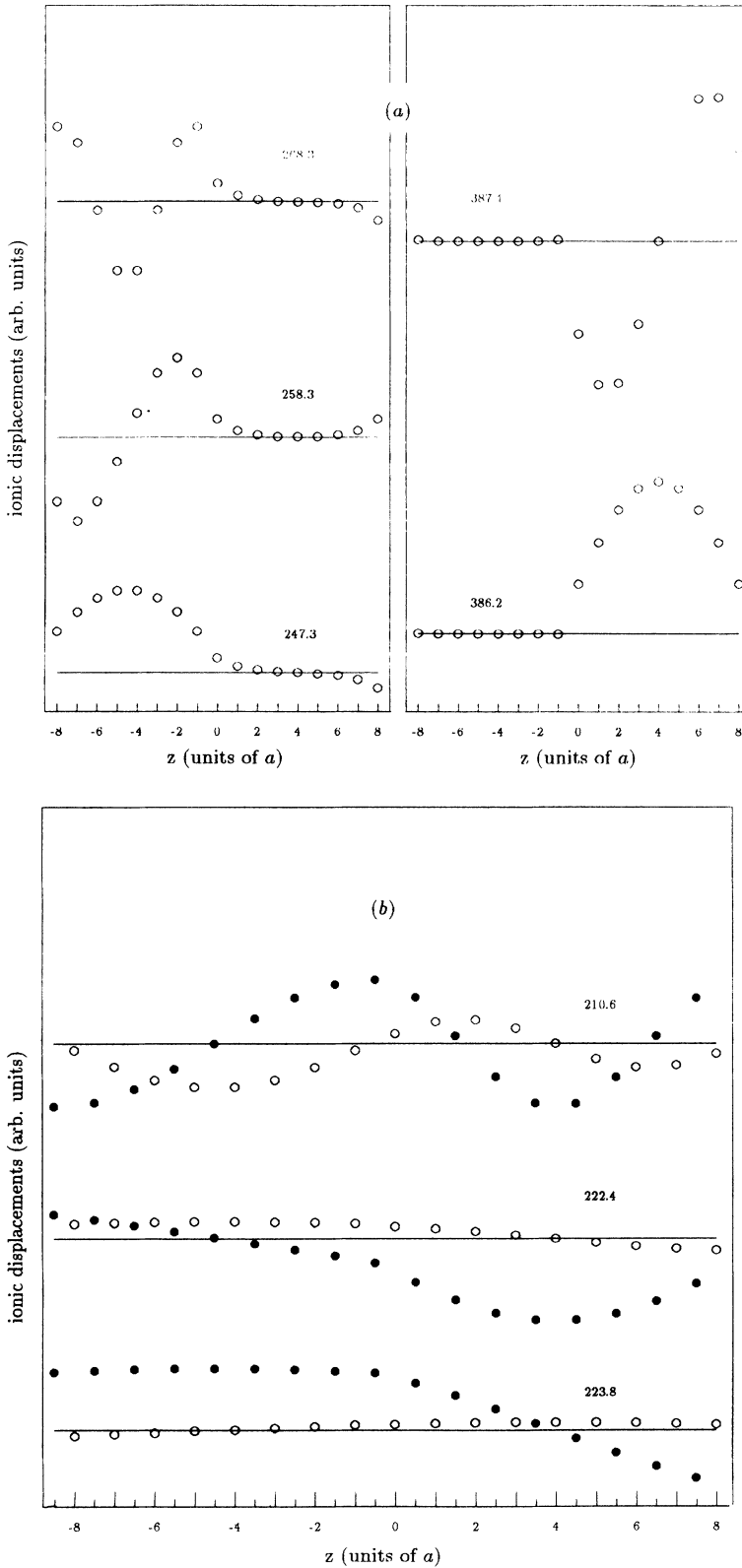
FIG. 2. The amplitudes of atomic displacements along the z direction in $(GaAs)_8/(AlAs)_9$ superlattice for the vibrations with $\mathbf{q}=(0,0)$, $Q=0$. Several modes bound to (a) LO and (b) LA bands are shown. Empty circles, $(-1)^m A_{z,NQ}^C[(0,0),m]$. In (b) displacements of the anions $(-1)^m A_{z,NQ}^A[(0,0),m]$ are also shown (filled circles). Figures near each graph are mode frequencies $\omega_{NQ}(0,0)$ in cm^{-1}.

ture. Electron states in these systems are described by a miniband number n and transverse wave number p: $\lambda = (n,p)$. Within the EFA, the electron energy spectrum and envelope functions for each valley can be easily obtained by the Kronig-Penney model. Generally speaking, this model must be improved in order to take into account Γ-X mixing effects. However, *first-order* calculation of $W^{\Gamma X_x(\pm)}_{\lambda,\lambda'}(\mathbf{k},\mathbf{k}')$ and $W^{\Gamma X_z(\pm)}_{\lambda,\lambda'}(\mathbf{k},\mathbf{k}')$ need not take

into account the influence of Γ-X mixing on the electron states, for Γ-X mixing itself can be considered as a perturbation. Therefore, we will use the simple Kronig-Penney model (without Γ-X mixing) for the calculation of phonon-assisted transfer probabilities.

Taking into account (14) and (22), it is convenient to rewrite (38) and (39) in the following way:

$$W^{\Gamma X_x(\pm)}_{np,n'p'}(\mathbf{k},\mathbf{k}') = \sum_{N,Q} \frac{\pi \overline{D}^2_X}{\omega_{NQ}(\pi/a,0)\overline{\rho}V} \delta_{p'-p,Q} |E^x_{NQ}(np\mathbf{k},n'p'\mathbf{k}')|^2$$

$$\times [N_{NQ}(\pi/a,0) + \tfrac{1}{2} \pm \tfrac{1}{2}] \delta(\epsilon^\Gamma_{np}(\mathbf{k}) - \epsilon^{X_x}_{n'p'}(\mathbf{k}') \mp \hbar\omega_{NQ}(\pi/a,0)) , \qquad (40)$$

$$W^{\Gamma X_z(\pm)}_{np,n'p'}(\mathbf{k},\mathbf{k}') = \sum_{N,Q} \frac{\pi \overline{D}^2_X}{\omega_{NQ}(0,0)\overline{\rho}V} \delta_{p'-p,Q} |E^z_{NQ}(np\mathbf{k},n'p'\mathbf{k}')|^2$$

$$\times [N_{NQ}(0,0) + \tfrac{1}{2} \pm \tfrac{1}{2}] \delta(\epsilon^\Gamma_{np}(\mathbf{k}) - \epsilon^{X_z}_{n'p'}(\mathbf{k}') \mp \hbar\omega_{NQ}(0,0)) , \qquad (41)$$

where

$$E^x_{NQ}(np\mathbf{k},n'p'\mathbf{k}') = \frac{1}{M_1+M_2} \sum_{m=-M_1}^{M_2-1} \left[\frac{M^m_C}{M^m_C+M_A} \right]^{1/2} \frac{D^m_X}{\overline{D}_X} F^\Gamma_{np\mathbf{k}}(ma)F^{X_x*}_{n'p'\mathbf{k}'}(ma)\tilde{A}^C_{x,NQ}[(\pi/a,0),m] , \qquad (42)$$

$$E^z_{NQ}(np\mathbf{k},n'p'\mathbf{k}') = \frac{1}{M_1+M_2} \sum_{m=-M_1}^{M_2-1} \left[\frac{M^m_C}{M^m_C+M_A} \right]^{1/2} \frac{D^m_X}{\overline{D}_X} F^\Gamma_{np\mathbf{k}}(ma)F^{X_z*}_{n'p'\mathbf{k}'}(ma)(-1)^m \tilde{A}^C_{z,NQ}[(0,0),m] . \qquad (43)$$

In (40)–(43) $\overline{\rho} = \overline{M}/[2a^3(M_1+M_2)]$ is the averaged density of the superlattice material, $\overline{M} = M_1(M_{C1}+M_A)+M_2(M_{C2}+M_A)$, $\overline{D}_X = (D_{1X}M_1+D_{2X}M_2)/(M_1+M_2)$ is the average Γ-X DP constant, V is the normalization volume, $D^m_X = D_{1X}$ for $m \in$ GaAs, and $D^m_X = D_{2X}$ for $m \in$ AlAs. Dimensionless "amplitudes" $\tilde{A}^s_{\alpha,NQ}(\mathbf{q},m) = \sqrt{S\omega_{NQ}(\mathbf{q})\overline{M}/(\hbar a^2)}A^s_{\alpha,NQ}(\mathbf{q},m)$ obey normalization conditions

$$\sum_{m=-M_1}^{M_2-1} (M^m_C\{|\tilde{A}^C_{x,NQ}[(\pi/a,0),m]|^2$$

$$+|\tilde{A}^C_{y,NQ}[(\pi/a,0),m]|^2\}$$

$$+M_A|\tilde{A}^A_{z,NQ}[(\pi/a,0),m]|^2) = \overline{M} , \qquad (44)$$

$$\sum_{m=-M_1}^{M_2-1} \{M^m_C|\tilde{A}^C_{z,NQ}[(0,0),m]|^2$$

$$+M_A|\tilde{A}^A_{z,NQ}[(0,0),m]|^2\} = \overline{M} , \qquad (45)$$

while electron envelope functions are normalized by the equations

$$\int_0^d dz |F^i_{np\mathbf{k}}(z)|^2 = d$$

or   (46)

$$\sum_{m=-M_1}^{M_2-1} |F^i_{np\mathbf{k}}(ma)|^2 = M_1 + M_2 .$$

Equations (40)–(46) together with the equations of Sec. III and the Appendix give us the complete solution of the

problem of phonon-assisted Γ-X transfer in (001)-grown GaAs/AlAs superlattices or MQW's. However, this solution implies a rather complicated procedure of the phonon spectrum determination. It is not convenient for the calculation of the phonon-assisted Γ-X transfer probability. To make the calculation easier, we notice that the main contribution in the overlap sums (42) and (43) arises from certain phonon modes: displacement patterns $\tilde{A}^C_{x,NQ}[(\pi/a,0),m],(-1)^m\tilde{A}^C_{z,NQ}[(0,0),m]$ for these modes have periods of oscillations greater than (or comparable with) the typical spatial scales of envelope products $F^\Gamma_{np\mathbf{k}}(z)F^{X_x*}_{n'p'\mathbf{k}'}(z), F^\Gamma_{np\mathbf{k}}(z)F^{X_z*}_{n'p'\mathbf{k}'}(z)$. These typical scales are great in comparison with the monolayer width a (provided that $M_1,M_2 \gg 1$). Therefore, the main contribution in E^x_{NQ} arises from several LO-bound GaAs- and AlAs-like phonons with smallest q_1 and q_2: $q_1 \ll \pi/a$, or $q_2 \ll \pi/a$ (see Fig. 1 for an illustration). In a similar way, the main contribution in E^z_{NQ} arises from LO-bound GaAs-like and AlAs-like phonons with the largest real q_1 and q_2: $|q_1 - \pi/a| \ll \pi/a$ or $|q_2 - \pi/a| \ll \pi/a$ (see Fig. 2). The frequencies of these phonons are close to the X-point LO frequencies of bulk GaAs and AlAs. Solution of Eq. (23) for LO-bound GaAs-like (or AlAs-like) modes in the limit of small q_1 (or q_2) shows that $q_1 \cong \pi L/(aM_1)$ [or $q_2 \cong \pi L/(aM_2)$], and

$$A^C_{x,NQ}[(\pi/a,0),m] \sim \sin(\pi Lm/M_1) ,$$

$$m = -1,-2,\ldots,M_1$$

or

$$A^C_{x,NQ}[(\pi/a,0),m] \sim \sin(\pi Lm/M_2), \quad m = 0,1,\ldots,M_2 ,$$

where $L = 1, 2, \ldots$. The solution of Eq. (33) for LO-bound GaAs (or AlAs) -like modes in the limit $|q_1 - \pi/a| \ll \pi/a$ (or $|q_2 - \pi/a| \ll \pi/a$) gives

$$(-1)^m A^C_{z,NQ}[(0,0),m] \sim \sin(\pi L m / M_1) ,$$

$$m = -1, -2, \ldots, -M_1$$

or

$$(-1)^m A^C_{z,NQ}[(0,0),m] \sim \sin(\pi L m / M_2),$$

$$m = 0, 1, \ldots, M_2 .$$

The same behavior is visible from Figs. 1(a) and 2(a), as already mentioned.

In the following, we take the approximations $\omega_{NQ}(0,0), \omega_{NQ}(\pi/a,0) \cong \omega_{1X}$ for a GaAs-like group of phonons and $\omega_{NQ}(0,0), \omega_{NQ}(\pi/a,0) \cong \omega_{2X}$ for an AlAs-like group, where ω_{1X}, ω_{2X} are the X-point LO frequencies of bulk GaAs and AlAs, respectively. We also neglect the dependence of all values in (40) and (41) on Q, because it is a very good approximation for LO-bound phonons. Finally, we again take into account that the electron envelope functions do not change considerably on a microscopic scale and transform overlap sums (42) and (43) into overlap integrals. Instead of (40) and (41) we obtain

$$W^{\Gamma X_x(\pm)}_{np,n'p'}(\mathbf{k},\mathbf{k}') = \frac{2\pi D^2_{1X} d}{\omega_{1X}\rho_1 V d_1} \sum^{\infty}_{L=1} \left| \frac{1}{d} \int^0_{-d_1} dz \, F^{\Gamma}_{np\mathbf{k}}(z) F^{X_x *}_{n'p'\mathbf{k}'}(z) \sin(\pi L z / d_1) \right|^2 (N_{1X} + \tfrac{1}{2} \pm \tfrac{1}{2}) \delta(\epsilon^{\Gamma}_{np}(\mathbf{k}) - \epsilon^{X_x}_{n'p'}(\mathbf{k}') \mp \hbar\omega_{1X})$$

$$+ \frac{2\pi D^2_{2X} d}{\omega_{2X}\rho_2 V d_2} \sum^{\infty}_{L=1} \left| \frac{1}{d} \int^{d_2}_0 dz \, F^{\Gamma}_{np\mathbf{k}}(z) F^{X_x *}_{n'p'\mathbf{k}'}(z) \sin(\pi L z / d_2) \right|^2$$

$$\times (N_{2X} + 1/2 \pm 1/2) \delta(\epsilon^{\Gamma}_{np}(\mathbf{k}) - \epsilon^{X_x}_{n'p'}(\mathbf{k}') \mp \hbar\omega_{2X}) , \qquad (47)$$

$$W^{\Gamma X_z(\pm)}_{np,n'p'}(\mathbf{k},\mathbf{k}') = \frac{2\pi D^2_{1X} d}{\omega_{1X}\rho_1 V d_1} \sum^{\infty}_{L=1} \left| \frac{1}{d} \int^0_{-d_1} dz F^{\Gamma}_{np\mathbf{k}}(z) F^{X_z *}_{n'p'\mathbf{k}'}(z) \sin(\pi L z / d_1) \right|^2 (N_{1X} + \tfrac{1}{2} \pm \tfrac{1}{2}) \delta(\epsilon^{\Gamma}_{np}(\mathbf{k}) - \epsilon^{X_z}_{n'p'}(\mathbf{k}') \mp \hbar\omega_{1X})$$

$$+ \frac{2\pi D^2_{2X} d}{\omega_{2X}\rho_2 V d_2} \sum^{\infty}_{L=1} \left| \frac{1}{d} \int^{d_2}_0 dz \, F^{\Gamma}_{np\mathbf{k}}(z) F^{X_z *}_{n'p'\mathbf{k}'}(z) \sin(\pi L z / d_2) \right|^2 (N_{2X} + \tfrac{1}{2} \pm \tfrac{1}{2}) \delta(\epsilon^{\Gamma}_{np}(\mathbf{k}) - \epsilon^{X_z}_{n'p'}(\mathbf{k}') \mp \hbar\omega_{2X}) ,$$

$$(48)$$

where $d_1 = aM_1$ and $d_2 = aM_2$ are the widths of the GaAs and AlAs layers, ρ_1 and ρ_2 are the densities of GaAs and AlAs, respectively, $N_{1X} = [\exp(\hbar\omega_{1X}/T) - 1]^{-1}$, and $N_{2X} = [\exp(\hbar\omega_{2X}/T) - 1]^{-1}$. Keeping in mind that the main contribution in the first and second terms of Eqs. (47) and (48) corresponds to $L \ll M_1$ and $L \ll M_2$, respectively, we have spread the summation over L in these equations to the infinity.

The rate of phonon-assisted electron transfer from Γ states to X states in GaAs/AlAs superlattices and MQW structures is given by the equation

$$\frac{1}{\tau^{ph}_{\Gamma X}} = \frac{2}{N_\Gamma V} \sum_{n,p,\mathbf{k}} \sum_{n',p',\mathbf{k}'} f^{\Gamma}_{np}(\mathbf{k})[\, 2W^{\Gamma X_x(+)}_{np,n'p'}(\mathbf{k},\mathbf{k}')$$

$$+ 2W^{\Gamma X_x(-)}_{np,n'p'}(\mathbf{k},\mathbf{k}')$$

$$+ W^{\Gamma X_z(+)}_{np,n'p'}(\mathbf{k},\mathbf{k}')$$

$$+ W^{\Gamma X_z(-)}_{np,n'p'}(\mathbf{k},\mathbf{k}')] , \qquad (49)$$

where $f^{\Gamma}_{np}(\mathbf{k})$ is the distribution function of the Γ electrons and

$$N_\Gamma = \frac{2}{V} \sum_{n,p,\mathbf{k}} f^{\Gamma}_{np}(\mathbf{k}) \qquad (50)$$

is the Γ-electron concentration in the system. The total Γ-X transfer rate $1/\tau_{\Gamma X}$ is described by the equation

$$\frac{1}{\tau_{\Gamma X}} = \frac{1}{\tau^{ph}_{\Gamma X}} + \frac{1}{\tau^0_{\Gamma X}} , \qquad (51)$$

where

$$\frac{1}{\tau^0_{\Gamma X}} = \frac{2}{N_\Gamma V} \sum_{n,p,\mathbf{k}} \sum_{n',p',\mathbf{k}'} f^{\Gamma}_{np}(\mathbf{k}) W^{\Gamma X_z(0)}_{np,n'p'}(\mathbf{k},\mathbf{k}') . \qquad (52)$$

Here $W^{\Gamma X_z(0)}_{np,n'p'}(\mathbf{k},\mathbf{k}')$ is the Γ-X transfer probability due to Γ-X mixing. We evaluate this probability with the use of the simplest model of Γ-X mixing proposed by Liu.[9] In this model, mixing between Γ and X envelope functions at the interfaces is described by a single parameter $\alpha \simeq 0.015$ eV nm (the given value is established by a comparison of the measured and calculated tunnel current through the AlAs barrier[5]). We have

$$W^{\Gamma X_z(0)}_{np,n'p'}(\mathbf{k},\mathbf{k}') = \frac{2\pi\alpha^2}{\hbar d^2} \delta_{\mathbf{k},\mathbf{k}'} \delta_{p,p'}$$

$$\times | F^{\Gamma}_{np\mathbf{k}}(-d_1) F^{X_z *}_{n'p'\mathbf{k}'}(-d_1)$$

$$- F^{\Gamma}_{np\mathbf{k}}(0) F^{X_z *}_{n'p'\mathbf{k}'}(0)|^2$$

$$\times \delta(\epsilon^{\Gamma}_{np}(\mathbf{k}) - \epsilon^{X_z}_{n'p'}(\mathbf{k}')) . \qquad (53)$$

In the remaining part of this section we will calculate $1/\tau^{ph}_{\Gamma X}$ and $1/\tau^0_{\Gamma X}$ in the application to the problem of Γ-X relaxation of photoexcited electrons in the type-II

GaAs/AlAs superlattices and MQW's. The calculated transfer rates will be compared with the experimental data (most of the data are summarized in Ref. 2).

We put $n = 1$ in Eqs. (49), (50), and (52) because only the lowest Γ-electron miniband is populated by the electrons due to the large energy spacing between the Γ-electron minibands in the type-II GaAs/AlAs superlattices. It should be noted that the Γ-electron distribution function $f_{np}^\Gamma(\mathbf{k})$ in these systems differs from the equilibrium distribution function because photoexcited electrons do not relax to thermal equilibrium prior to Γ-X transfer (experiments[2,13,25] show that the Γ-X transfer times are on a picosecond or even subpicosecond scale). Although $f_{np}^\Gamma(\mathbf{k})$ is not known exactly, we approximate it by the Boltzmann distribution function with a single parameter—the effective electron temperature T_e.

The values of phonon-assisted Γ-X transfer rates $1/\tau_{\Gamma X}^{ph}$, together with the values of the Γ-X mixing-induced transfer rates $1/\tau_{\Gamma X}^0$ calculated from the Eqs. (47)–(50), (52), and (53), are plotted in Figs. 3 and 4. We use the following parameters of the GaAs/AlAs system: the Γ-valley energy offset $V_\Gamma = 1.0$ eV; the X-valley energy offset $V_X = 0.3$ eV; the energy difference between the X-valley bottom in AlAs and the Γ-valley bottom in GaAs, $V_0 = 0.18$ eV (it should be noted that in different papers value of V_0 varies between 0.15 and 0.20 eV). The Γ-electron mass, the longitudinal X-electron mass, and the transverse X-electron mass of GaAs are $0.067m_0$, $1.3m_0$, and $0.24m_0$, respectively (here m_0 is the free electron mass); the corresponding AlAs effective masses are $0.10m_0$, $1.1m_0$, and $0.19m_0$, $\rho_1 = 5.316$ g/cm^3, $\rho_2 = 3.76$ g/cm^3, $\omega_{1X} = 0.030$ eV, $\omega_{2X} = 0.048$ eV, and
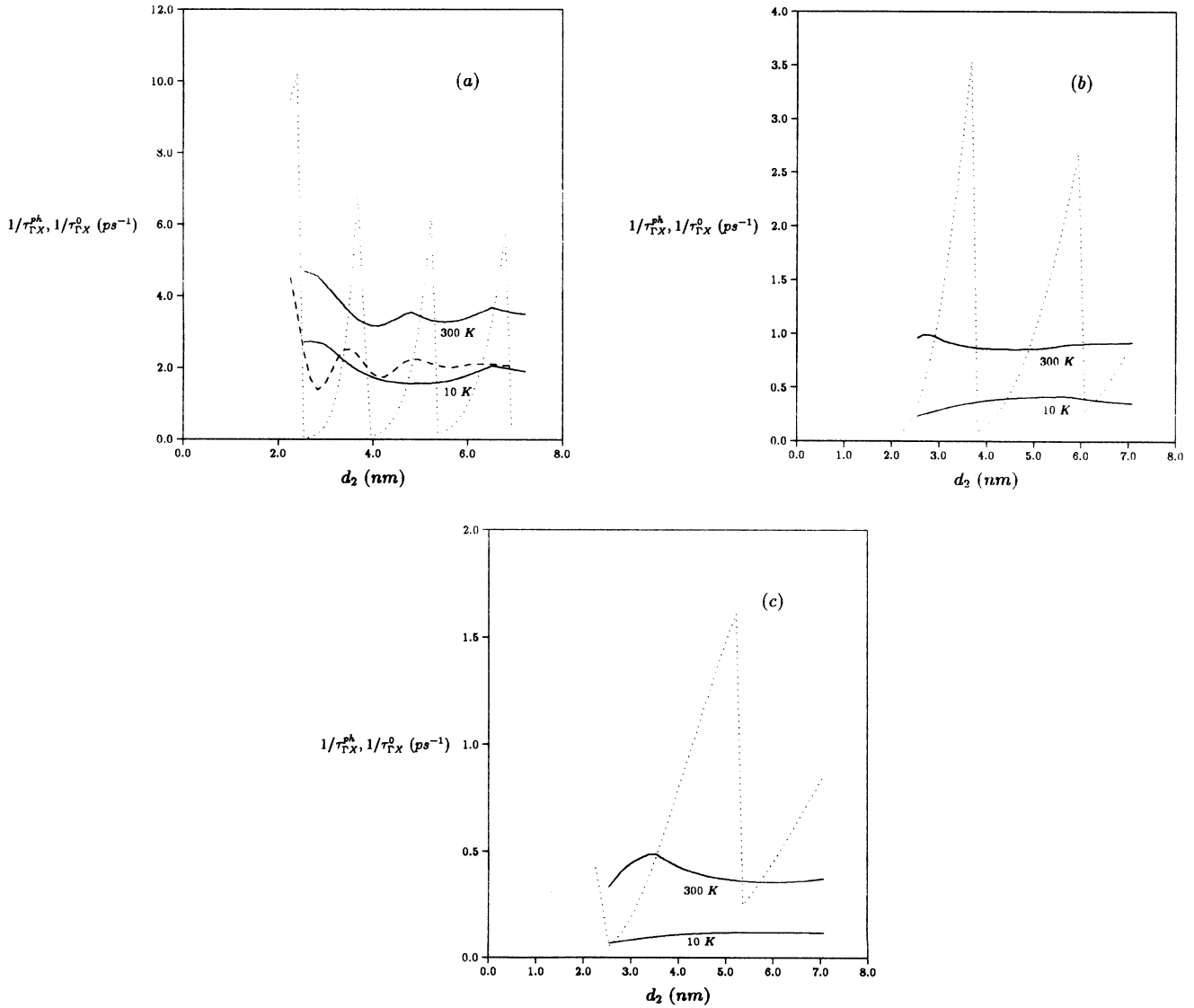
FIG. 3. Γ-X transfer rates in (GaAs)$_{M_1}$/(AlAs)$_{M_2}$ superlattices as functions of the AlAs layer thickness $d_2 = aM_2$ at $T_e = 300$ K: (a) $M_1 = 8$($d_1 = 2.264$ nm); (b) $M_1 = 10$ ($d_1 = 2.83$ nm); (c) $M_1 = 11$($d_1 = 3.113$ nm). Solid lines, $1/\tau_{\Gamma X}^{ph}$ at $T = 300$ and 10 K; dotted lines, $1/\tau_{\Gamma X}^0$. In (a) the dashed line corresponds to $1/\tau_{\Gamma X}^0$ for the imperfect superlattice (see text for explanation).

$D_{1X} = D_{2X} = 10^9$ eV/cm. We note that there is some discrepancy in the values of Γ-X intervalley DP constants obtained by different authors. Pseudopotential calculation[26] gives $D_{1X} = 0.41 \times 10^9$ eV/cm and $D_{2X} = 0.44 \times 10^9$ eV/cm, while recent experiment[27] gives $D_{1X} = 1.07 \times 10^9$ eV/cm. Keeping in mind that the typical values of the Γ-X intervalley DP constants being used in high-field transport theories are 10^9 eV/cm, we use these values both for GaAs and for AlAs.

Figure 3 shows that the phonon-assisted Γ-X transfer rate $1/\tau_{\Gamma X}^{ph}$ exhibits a weak dependence on the AlAs layer width d_2 because a reduction in the overlap between Γ and X envelope functions due to increase of d_2 is partly compensated for by the increase in X-electron density of states. Weak oscillations [clearly visible in Fig. 3(a)] reflect the involvement of more X-electron minibands in the scattering process. On the other hand, the dependence of $1/\tau_{\Gamma X}^{ph}$ on the GaAs layer thickness d_1 [compare Figs. 3(a)–3(c)] shows a pronounced decrease because the reduction in the Γ-X overlap is no longer compensated for by the increase in the X-electron density of states. This behavior is in good agreement with the experiment.[2] From Figs. 3 and 4 we can see that $1/\tau_{\Gamma X}^{ph}$ increases with an increase of lattice temperature T and electron temperature T_e. This behavior can be explained mostly as a result of involving of more X states in scattering. We note that $1/\tau_{\Gamma X}^{ph}$ for the $(GaAs)_{11}/(AlAs)_{24}$ superlattice is close to zero at low T and T_e [Fig. 4(c)], because energy spacing between the lowest Γ and X_z minibands in this system appeared to be smaller than the GaAs intervalley phonon energy $\hbar\omega_{1X}$. As a rule, experiment[2] also shows an increase of the Γ-X transfer times with an increase of lattice temperature.

The dotted lines in Figs. 3 and 4 represent the behavior of the Γ-X mixing transfer rate $1/\tau_{\Gamma X}^0$. Due to a **k** conservation law in (53), $1/\tau_{\Gamma X}^0$ oscillates with d_2, the maximums occur when the energy of the n'th X_z-electron miniband is close to the energy of the first Γ-electron miniband. For example, four peaks in Fig. 1(a) correspond to $n' = 2, 3, 4, 5$. It should be noted, however, that such sharp oscillation picture is unlikely to be observed experimentally because scattering and disorder due to the imperfect fabrication would considerably damp it. To demonstrate this phenomenon, we calculated $1/\tau_{\Gamma X}^0$ for the imperfect superlattice [Fig. 4(a), dashed line]. We assumed that the interface positions fluctuate from layer to layer, and the amplitudes of the fluctuations obey a Gaussian distribution law with variance equal to a 0.25 monolayer thickness. Although such fluctuations have no serious effect on the phonon-assisted Γ-X transfer rates, the oscillations of the Γ-X mixing transfer rate become significantly damped.

A comparison of the absolute values of $1/\tau_{\Gamma X}^{ph}$ and $1/\tau_{\Gamma X}^0$ shows that both the phonon-assisted Γ-X transfer and the transfer due to Γ-X mixing are important. The calculated values of the total Γ-X transfer rates $1/\tau_{\Gamma X}$ are close enough to the experimental values[2] [compare, for example, the results for the structures $(GaAs)_8/(AlAs)_9$, $(GaAs)_{10}/(AlAs)_{17}$, and $(GaAs)_{11}/(AlAs)_{24}$].
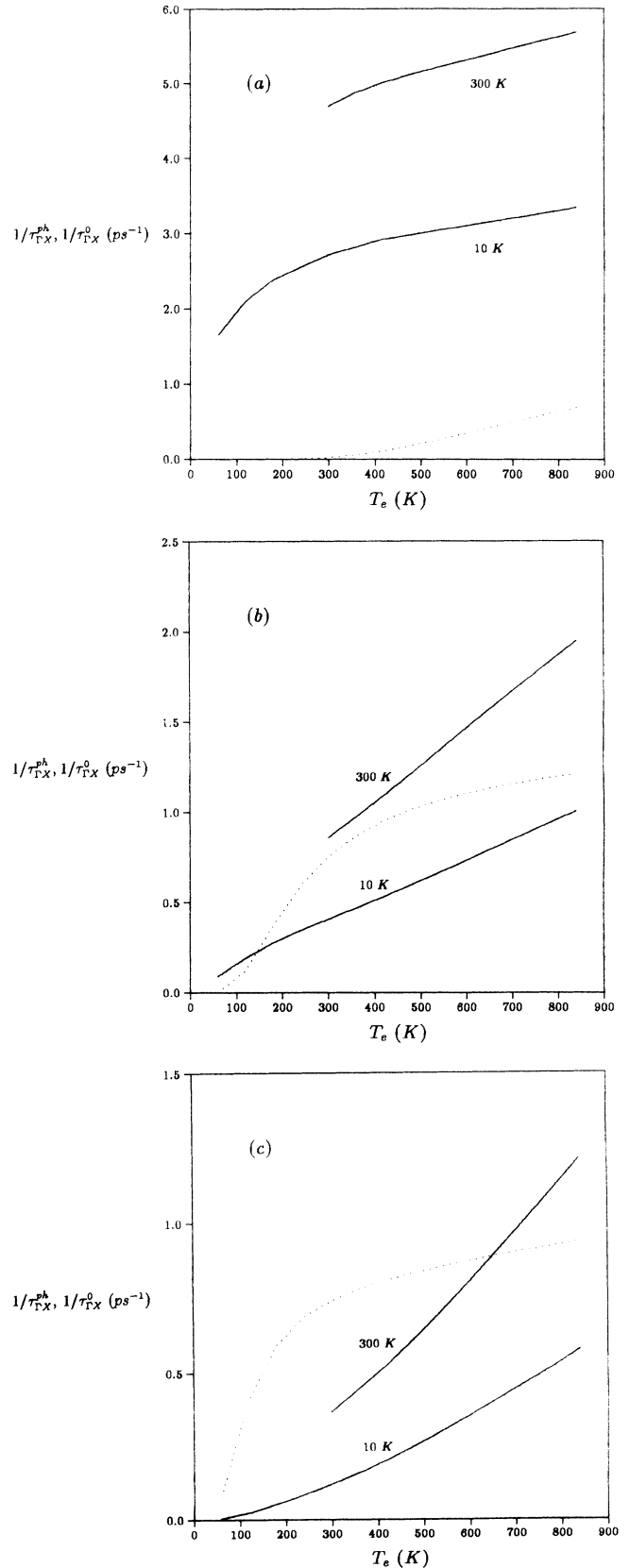
FIG. 4. Γ-X transfer rates in $(GaAs)_{M_1}/(AlAs)_{M_2}$ superlattices as functions of the electron temperature T_e: (a) $M_1 = 8$, $M_2 = 9$; (b) $M_1 = 10, M_2 = 17$; (c) $M_1 = 11$, $M_2 = 24$. Solid lines, $1/\tau_{\Gamma X}^{ph}$ at $T = 300$ and 10 K; dotted lines, $1/\tau_{\Gamma X}^0$.

V. CONCLUSIONS

In this paper we have developed a EFA-compatible theory of the phonon-assisted Γ-X transfer in the periodic GaAs/AlAs heterostructures (superlattices and MQWs) grown in the (001) direction. Using the EFA, we have shown that long-range (macroscopic) fields generated by the lattice vibrations are not important for the intervalley transitions of the electrons. Therefore, only the deformation-potential interaction is responsible for the Γ-X intervalley scattering in GaAs/AlAs heterostructures (as it is in bulk GaAs or AlAs). In this case the perturbation potential due to the lattice vibration can be considered to be local with respect to slowly varying envelope functions of Γ and X electrons. This property enabled us to express the matrix elements of the Γ-X intervalley transitions in heterostructures through the overlap sums of Γ- and X-envelope functions with amplitudes of atomic displacements, using *bulk* intervalley deformation potential constants of GaAs and AlAs [see (12) and (16)]. In order to determine these amplitudes, we have carried out microscopic calculations of the vibrational spectrum of an ideal GaAs/AlAs superlattice. We find that vibrational eigenmodes (phonons) responsible for intervalley Γ-X scattering of electrons are LO-bound GaAs-like and AlAs-like phonons confined in GaAs and AlAs layers, respectively. Frequencies of these phonons are close to X-point LO frequencies of bulk GaAs and AlAs. Taking into account the results of our microscopic calculations of lattice vibrations and using the properties of electron envelope functions, we have obtained simple expression for phonon-assisted Γ-X transfer probability.

The theory has been applied to the calculation of relaxation times of the photoexcited electrons in type-II GaAs/AlAs superlattices. Apart from the phonon-assisted Γ-X transfer, we have taken into account phononless Γ-X transfer due to the mixing of Γ and X states at the interfaces. These two mechanisms of transfer completely describe the case of an ideal GaAs/AlAs heterostructure and must always be taken into account. (Additional Γ-X transfer mechanisms may arise in nonideal or alloy-containing heterostructures.) A comparison of the phonon-assisted Γ-X transfer rates with the transfer rates due to Γ-X mixing shows that both mechanisms are important for the description of Γ-X transfer in the heterostructures. Calculated values of the transfer times and their dependence on layer thicknesses are in agreement with the experimental data. Both the experiment and the theory show that Γ-X transfer times in GaAs/AlAs superlattices with rather thin layers are on a subpicosecond scale. This property provides the possibility for the application of these structures in the development of new high-speed real-space transfer devices.

APPENDIX

Boundary conditions for the determination of the constants $A_1^+, A_1^-, B_1^+, B_1^-, A_2^+, A_2^-, B_2^+, B_2^-$ from (28) can be obtained from the analysis of Eq. (23) in the vicinity of interfaces. We have

$$v_{A1}^+ + v_{A1}^- + v_{B1}^+ + v_{B1}^- = v_{A2}^+ + v_{A2}^- + v_{B2}^+ + v_{B2}^- , \tag{A1}$$

$$v_{A1}^+ e^{-iq_1 a} + v_{A1}^- e^{iq_1 a} - v_{B1}^+ e^{-iq_1 a} - v_{B1}^- e^{iq_1 a} = v_{A2}^+ e^{-iq_2 a} + v_{A2}^- e^{iq_2 a} - v_{B2}^+ e^{-iq_2 a} - v_{B2}^- e^{iq_2 a} , \tag{A2}$$

$$e^{iQd}(v_{A1}^+ e^{-iq_1 aM_1} + v_{A1}^- e^{iq_1 aM_1} + v_{B1}^+ (-1)^{M_1} e^{-iq_1 aM_1} + v_{B1}^- (-1)^{M_1} e^{iq_1 aM_1})$$
$$= v_{A2}^+ e^{iq_2 aM_2} + v_{A2}^- e^{-iq_2 aM_2} + v_{B2}^+ (-1)^{M_2} e^{iq_2 aM_2} + v_{B2}^- (-1)^{M_2} e^{-iq_2 aM_2} , \tag{A3}$$

$$e^{iQd}(v_{A1}^+ e^{-iq_1 a(M_1+1)} + v_{A1}^- e^{iq_1 a(M_1+1)} - v_{B1}^+ (-1)^{M_1} e^{-iq_1 a(M_1+1)} - v_{B1}^- (-1)^{M_1} e^{iq_1 a(M_1+1)})$$
$$= v_{A2}^+ e^{iq_2 a(M_2-1)} + v_{A2}^- e^{-iq_2 a(M_2-1)} - v_{B2}^+ (-1)^{M_2} e^{iq_2 a(M_2-1)} - v_{B2}^- (-1)^{M_2} e^{-iq_2 a(M_2-1)} , \tag{A4}$$

where vector v is defined in the following way:

$$v_{A1}^\pm = A_1^\pm \begin{bmatrix} 1 \\ \pm\lambda_1 \end{bmatrix}, \quad v_{A2}^\pm = A_2^\pm \begin{bmatrix} 1 \\ \pm\lambda_2 \end{bmatrix}, \quad v_{B1}^\pm = B_1^\pm \begin{bmatrix} \pm\lambda_1 \\ 1 \end{bmatrix}, \quad v_{B2}^\pm = B_2^\pm \begin{bmatrix} \pm\lambda_2 \\ 1 \end{bmatrix}, \tag{A5}$$

Q is the transverse wave number of the atomic vibrations in the superlattice and $d = a(M_1 + M_2)$ is the superlattice period. Equations (A3) and (A4) have been obtained with the use of the Bloch conditions $A_{\alpha,NQ}^s[q, m + n(M_1 + M_2)] = \exp(iQdn)A_{\alpha,NQ}^s(q, m)$.

In similar way, boundary conditions for the determination of $A_1^+, A_1^-, B_1^+, B_1^-, A_2^+, A_2^-, B_2^+, B_2^-$ from (35) are

$$v_{A1}^+ + v_{A1}^- + v_{B1}^+ + v_{B1}^- = v_{A2}^+ + v_{A2}^- + v_{B2}^+ + v_{B2}^- , \tag{A6}$$

$$v_{A1}^+ e^{-iq_1^+ a} + v_{A1}^- e^{iq_1^+ a} + v_{B1}^+ e^{-iq_1^- a} + v_{B1}^- e^{iq_1^- a} = v_{A2}^+ e^{-iq_2^+ a} + v_{A2}^- e^{iq_2^+ a} + v_{B2}^+ e^{-iq_2^- a} + v_{B2}^- e^{iq_2^- a} , \tag{A7}$$

$$e^{iQd}(v_{A1}^{+}e^{-iq_1^{+}aM_1}+v_{A1}^{-}e^{iq_1^{+}aM_1}+v_{B1}^{+}e^{-iq_1^{-}aM_1}+v_{B1}^{-}e^{iq_1^{-}aM_1})$$

$$=v_{A2}^{+}e^{iq_2^{+}aM_2}+v_{A2}^{-}e^{-iq_2^{+}aM_2}+v_{B2}^{+}e^{iq_2^{-}aM_2}+v_{B2}^{-}e^{-iq_2^{-}aM_2}, \qquad (A8)$$

$$e^{iQd}(v_{A1}^{+}e^{-iq_1^{+}a(M_1+1)}+v_{A1}^{-}e^{iq_1^{+}a(M_1+1)}+v_{B1}^{+}e^{-iq_1^{-}a(M_1+1)}+v_{B1}^{-}e^{iq_1^{-}a(M_1+1)})$$

$$=v_{A2}^{+}e^{iq_2^{+}a(M_2-1)}+v_{A2}^{-}e^{-iq_2^{+}a(M_2-1)}+v_{B2}^{+}e^{iq_2^{-}a(M_2-1)}+v_{B2}^{-}(-1)^{M_2}e^{-iq_2^{-}a(M_2-1)}. \qquad (A9)$$

where

$$v_{A1}^{\pm}=A_1^{\pm}\begin{bmatrix}\lambda_1^{+}\exp(\mp iq_1^{+}a/2)\\ 1\end{bmatrix}, \quad v_{A2}^{\pm}=A_2^{\pm}\begin{bmatrix}\lambda_2^{+}\exp(\mp iq_2^{+}a/2)\\ 1\end{bmatrix},$$

$$v_{B1}^{\pm}=B_1^{\pm}\begin{bmatrix}\lambda_1^{-}\exp(\mp iq_1^{-}a/2)\\ 1\end{bmatrix}, \quad v_{B2}^{\pm}=B_2^{\pm}\begin{bmatrix}\lambda_2^{-}\exp(\mp iq_2^{-}a/2)\\ 1\end{bmatrix}. \qquad (A10)$$

[1] T. Ando and A. Akera, Phys. Rev. B **40**, 11 619 (1989).

[2] J. Feldmann, J. Nunnenkamp, G. Peter, E. O. Göbel, J. Kuhl, K. Ploog, P. Dawson, and C. T. Foxon, Phys. Rev. B **42**, 5809 (1990).

[3] Z. S. Gribnikov and O. E. Raichev, Fiz. Tekh. Poluprovodn. **24**, 346 (1990) [Sov. Phys.—Semicond. **24**, 212 (1990)].

[4] Z. S. Gribnikov, K. Hess, and G. A. Kosinovsky, J. Appl. Phys. (to be published).

[5] D. Landheer, H. C. Liu, M. Buchanan, and R. Stoner, Appl. Phys. Lett. **54**, 1784 (1989).

[6] E. E. Mendez, E. Calleja, and W. I. Wang, Appl. Phys. Lett. **53**, 977 (1988).

[7] H. Schneider, K. von Klitzing, and K. Ploog, Superlatt. Microstruct. **5**, 383 (1989).

[8] O. E. Raichev, Fiz. Tekh. Poluprovodn. **25**, 1228 (1991) [Sov. Phys.—Semicond. **25**, 740 (1991)].

[9] H. C. Liu, Appl. Phys. Lett. **51**, 1019 (1987).

[10] Z. S. Gribnikov and O. E. Raichev, Fiz. Tekh. Poluprovodn. **23**, 2171 (1989) [Sov. Phys.—Semicond. **23**, 1344 (1989)].

[11] P. J. Price, Surf. Sci. **196**, 394 (1988).

[12] H. Kalt, W. W. Ruhle, and K. Reinmann, Solid State Electron. **32**, 1819 (1989).

[13] J. Feldmann, R. Sattmann, G. Peter, E. O. Göbel, J. Nunnenkamp, J. Kuhl, J. Hebling, K. Ploog, R. Cingolani, R. Muralidharan, P. Dawson, and C. T. Foxon, Surf. Sci. **229**, 452 (1990).

[14] A. M. de Paula, A. C. Maciel, M. C. Tatham, J. F. Ryan, P. Dawson, and C. T. Foxon, in *Proceedings of the 20th International Conference on the Physics of Semiconductors,* edited by J. D. Joannopoulos and E. Anastassakis (World Scientific, Singapore, 1990), p. 1421.

[15] B. A. Wilson, C. E. Bonner, R. C. Spitzer, R. Fischer, P. Dawson, K. J. Moore, C. T. Foxon, and G. W. 't Hooft, Phys. Rev. B **40**, 1825 (1989).

[16] A. S. Barker, J. L. Merz, and A. C. Gossard, Phys. Rev. B **17**, 3181 (1978).

[17] Sung-kit Yip and Yia-Chung Chang, Phys. Rev. B **30**, 7073 (1984).

[18] E. Molinari, A. Fasolino, and K. Kunc, Superlatt. Microstruct. **2**, 397 (1986).

[19] S. Baroni, P. Giannozzi, and E. Molinari, Phys. Rev. B **41**, 3870 (1990).

[20] E. Molinari, S. Baroni, P. Giannozzi, and S. de Gironcoli, in *Proceedings of the 20th International Conference on the Physics of Semiconductors* (Ref. 14), 1429.

[21] P. Lugli, E. Molinari, and H. Rücker, Superlatt. Microstruct. **10**, 471 (1991).

[22] M. Deans and J. C. Inkson, Semicond. Sci. Technol. **4**, 138 (1989).

[23] P. Giannozzi, S. de Gironcoli, P. Pavone, and S. Baroni, Phys. Rev. B **43**, 7231 (1991).

[24] Due to high symmetry of the point $\mathbf{q}=(\pi/a,0)$, $Q=0$, the amplitudes of the displacements can be chosen real and we do not need to plot separate graphs for real and imaginary parts. The same is true for the point $\mathbf{q}=(0,0)$, $Q=0$.

[25] J. Feldmann, R. Sattmann, E. O. Göbel, J. Kuhl, J. Hebling, K. Ploog, R. Muralidharan, P. Dawson, and C. T. Foxon, Phys. Rev. Lett. **62**, 1892 (1989).

[26] S. Zollner, S. Gopalan, and M. Cardona, Appl. Phys. Lett. **54**, 614 (1989).

[27] S. Satpathy, M. Chandrasekhar, H. R. Chandrasekhar, and U. Venkateswaran, Phys. Rev. B **44**, 11 339 (1991).